

Non-destructive analysis of pathological belemnite rostra by micro-CT techniques

RENÉ HOFFMANN, KEVIN STEVENS, MARIE-CLAIRE PICOLLIER, JÖRG MUTTERLOSE, and CHRISTIAN KLUG



Hoffmann, R., Stevens, K., Picollier, M.-C., Mutterlose, J., and Klug, C. 2020. Non-destructive analysis of pathological belemnite rostra by micro-CT techniques. *Acta Palaeontologica Polonica* 65 (1): 11–27.

Previously, palaeopathological features of fossil hardparts were often difficult to interpret because it was impossible to decipher their internal structure without destroying the specimens. We applied high-resolution computed-tomography (CT) to document such internal structures. This enabled us to describe a variety of pathologies of Jurassic and Cretaceous belemnite rostra. The examined rostra have been assigned to the taxa *Acrocoelites* sp., *Belemnellocomax* spp., *Belemnitella* sp., *Duvalia emerici*, *Goniocamax* sp., *Goniot euthis* spp., *Hibolites jaculoides*, *Neoclavibelus subclavatus*, and *Pseudobelus* sp. The studied pathologies comprise rostra with two apices, bulges, pearls, broken juvenile rostra, highly porous rostra with abnormal growth increments, blunt-rostra, rostra with callus-like structures, and bent- or knee-shaped rostra. In one rostrum the apex has been turned towards the anterior (alveolus) during ontogeny. Additionally, computed-tomography data were used to document diagenetic alterations of the rostra such as silification, sedimentary infill, pyrite formation. Specimens can also be tested for the presence or absence of internal elements (septa, siphuncle) and surface features. Palaeoecological studies clearly benefit from the application of computed-tomography to gain high resolution images of otherwise invisible internal features of extinct organisms, as demonstrated herein.

Key words: Cephalopoda, Belemnitida, palaeopathology, rostra, micro computed-tomography, diagenesis, Jurassic, Cretaceous, Germany.

René Hoffmann [rene.hoffmann@rub.de], Kevin Stevens [kevin.stevens@rub.de], and Jörg Mutterlose [joerg.mutterlose@rub.de], Institut für Geologie, Mineralogie und Geophysik, Ruhr-Universität Bochum, Universitätsstr. 150, 44801 Bochum, Germany.

Marie-Claire Picollier [mc.picollier@wanadoo.fr], La Vitonie, 24160 St. Pantaly d'Excideuil, France.

Christian Klug [chklug@pim.uzh.ch], Paläontologisches Institut und Museum, Universität Zürich, Karl-Schmid-Strasse 4, CH-8006 Zürich, Switzerland.

Received 14 October 2019, accepted 7 January 2020, available online 4 March 2020.

Copyright © 2020 R. Hoffmann et al. This is an open-access article distributed under the terms of the Creative Commons Attribution License (for details please see <http://creativecommons.org/licenses/by/4.0/>), which permits unrestricted use, distribution, and reproduction in any medium, provided the original author and source are credited.

Introduction

The term pathology refers to malformations of specimens of a population or species that are caused by exogenic or endogenic processes. Exogenic processes include injuries due to a predator attack, parasite infections, and the colonisation of the shell during lifetime (Davis et al. 1999). Endogenic processes include infections, mutations, or other illnesses (Buikstra et al. 2017). For describing pathological features of fossils, Shufeldt (1892) proposed the term palaeopathology. To ensure accurate palaeoecological interpretations it is required to distinguish between pathologies and pseudopathologies, e.g., tectonically deformed belemnite rostra (Fraas 1859). Fractures of tectonically deformed rostra are

filled with blocky calcite cement instead of biogenic radial fibrous calcite (Hoffmann et al. 2016). Such rostra, therefore, do not contribute to our understanding of belemnite palaeoecology (Hoffmann and Stevens 2019). The visible reactions of an affected specimen are called symptoms while several abnormalities that occur in a single specimen are described as complex syndromes such as, for instance, Morton's syndrome, which was described for ammonites by Landman and Waage (1986). As a rule, only reactions to the disturbing factor should be considered to characterize pathological symptoms or syndromes. The disturbing factor (pathogen) underlying the palaeopathological features of fossil hardparts is only rarely identified. In exceptional cases, specific bite traces with a distinct shape or morphology of shell breakage are preserved (Richter 2009; Keupp 2012;

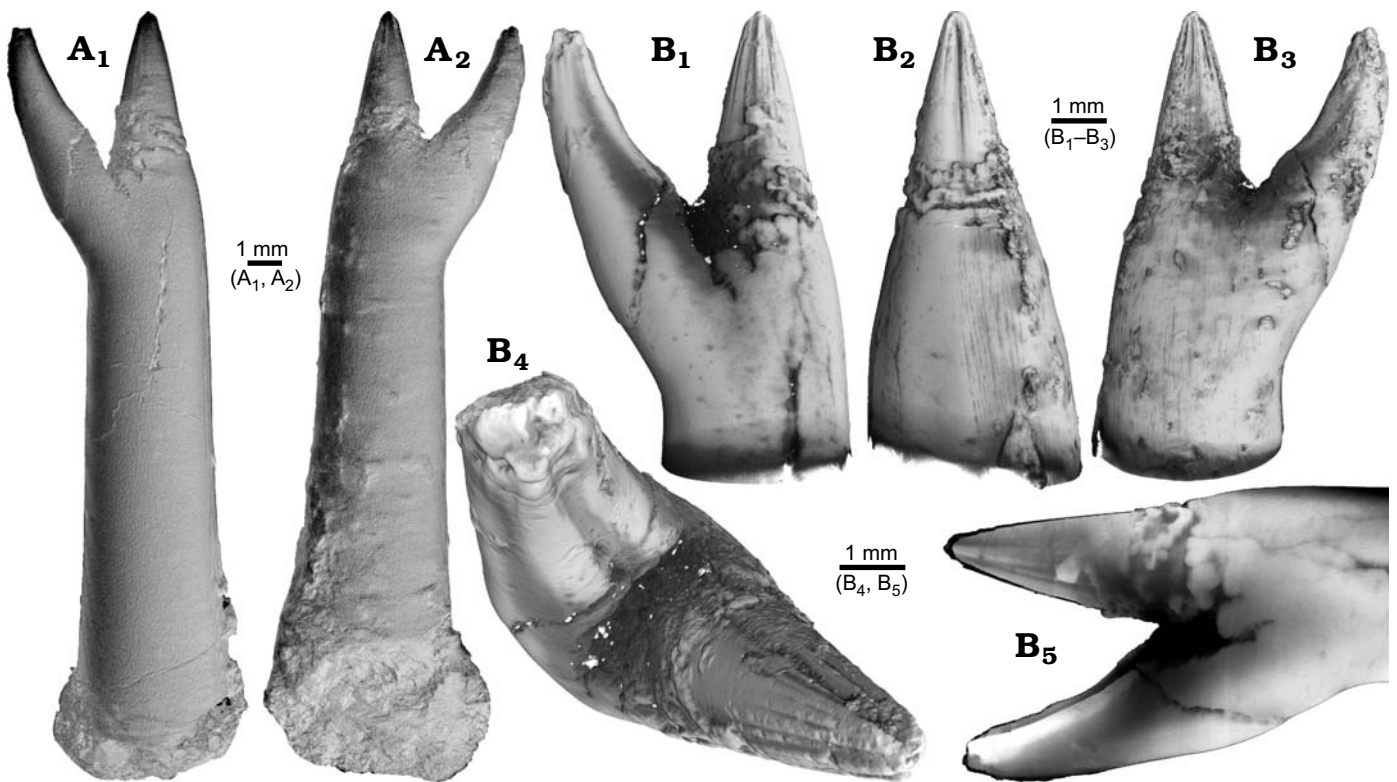


Fig. 1. Rostrum of belemnite *Acrocoelites* sp., PIMUZ 37346, Toarcian, Altdorf (SW-Germany) with forma aegra saepia (leg. M. Weissmüller). **A.** Overview (A_1, A_2). **B.** Close-up of the two apices, showing the radial furrows covering the apex that represent the “normal” tip of the rostrum (B_1 – B_3).

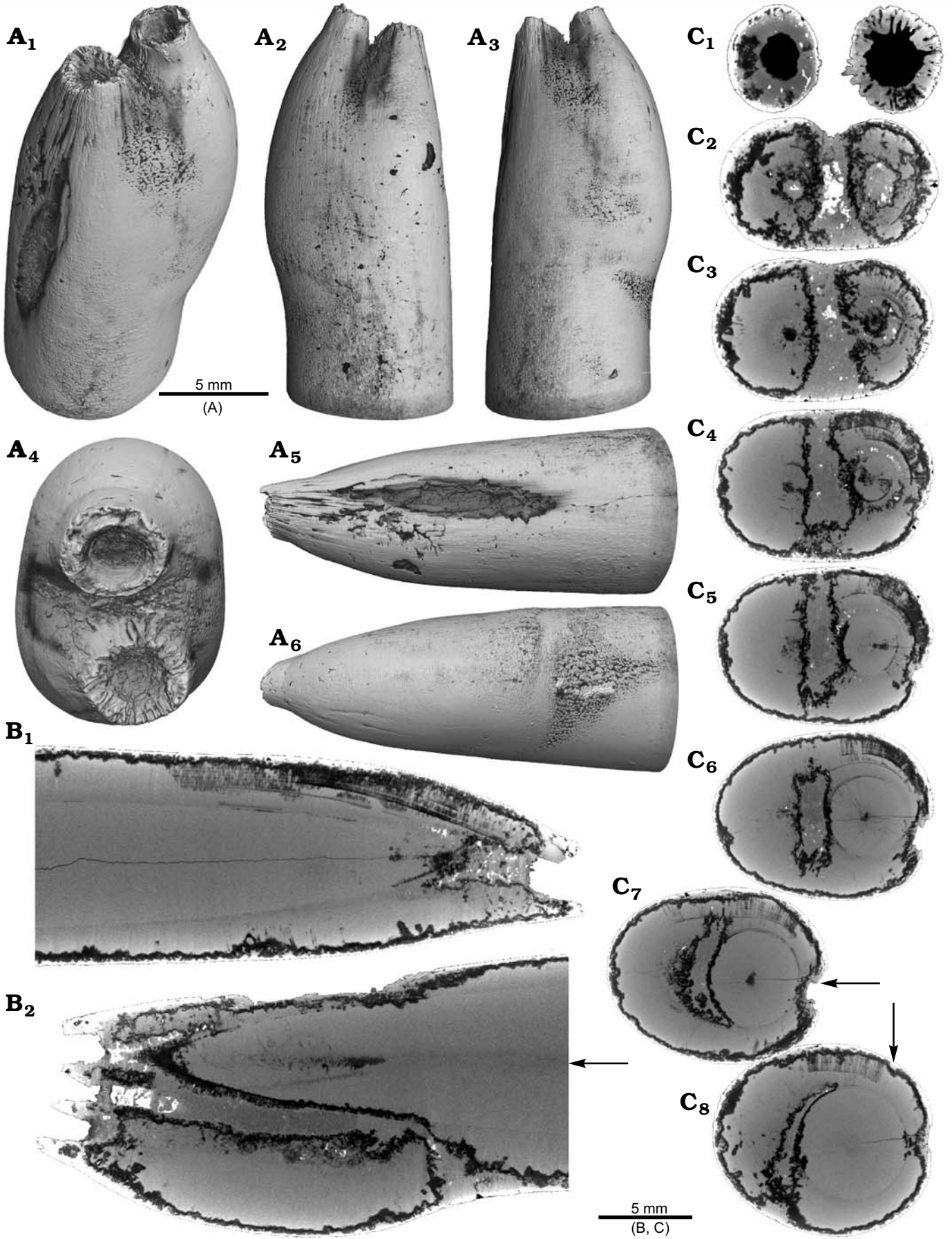
Hoffmann and Keupp 2015) and allow the identification of specific producers such as crustaceans, coleoids, fishes, or reptiles. Herein, we follow the suggestion of Vallon et al. (2015) to abandon the term bite mark for such phenomena and restrict the use of the term “mark” to physical (abiogenic) sedimentary structures, e.g., flute marks. The term “trace” is defined as a morphologically recurrent structure resulting from the life activity of organisms modifying the substrate (Bertling et al. 2006).

Pathologies of modern and fossil cephalopods have received proportionally large attention (e.g., Hengsbach 1996; Kröger 2000; Keupp 2000, 2012; Klug 2007; De Baets et al. 2011, 2015; Gestal et al. 2019). First reports on malformed cephalopods date back to Schröter (1774) although he did not recognise them as such. Later, pathological specimens were regarded as monstrous natural curiosities. Engel (1894) and Abel (1916) were the first to discuss potential factors causing abnormal morphologies. Consequently, exploration of the disturbing factors was increasingly used to reconstruct the palaeobiology and palaeoecology of the affected specimens and helped in reconstructing phylogenetic processes (e.g., Schindewolf 1934; Hölder 1956; Keupp 2000; Kröger 2000).

For belemnites, the earliest reports on pathological forms date back to Blainville (1827), Raspail (1829), Duval-Jouve (1841), d’Orbigny (1842), Schlüter (1876), and Wundt (1883). Quenstedt (1846–1849, 1858, described malformed rostra as “Krüppelformen”, “crippled forms”. Due to their internal shell, coleoid cephalopods such as belemnites are not affected by epizoans that settle on the external shells of nautiloids or ammonoids (Meischner 1968; Keupp 2012; Hoffmann and Keupp 2015). The assumption of a syn vivo infestation of belemnites by cirripeds (Seilacher 1968; Seilacher and Gishlick 2015) is rejected herein. These boring traces are seen here as a post mortem phenomenon due to the absence of any reaction of the hosting belemnite (Keupp 2012; Hoffmann and Stevens 2019). In externally shelled cephalopods, damage to the phragmocone can result in uncontrolled flooding of the chambers, which in turn leads to lethal drowning by shell implosion (see Kröger and Keupp 2004 and Tsujino and Shigeta 2012 for exceptions). In contrast, the internal shell of coleoids often remains in the mantle sac after being fractured. In case the animal survived the attack, damaged skeletal parts are often successfully repaired.

Data gained from palaeopathological studies of cepha-

Fig. 2. Rostrum of belemnite *Goniotenthis* sp., RUB-Pal 11264, Campanian, Höver (NW-Germany) with forma aegra saepia (leg. J. Bruns). **A.** Surface images showing the hollow opening of the two apices, and the partially dissolved or poorly mineralized rostrum (A_1 – A_6); arrow in A_5 indicates meandering trace fossil. **B.** Longitudinal section showing growth increments, apical line, and irregular mineralized layers (B_1, B_2). **C.** Cross sections with increasing distance to the apices (C_1 – C_8), showing the process of apex separation, only the straight continuous apex (arrows) develops distinct growth increments and the apical line (see also the arrow in B_2), note: the area between the apices is filled with sediment (diffuse grey area) and pyrite (white area), black area silicified.



lopods helped in estimating the efficiency of the buoyancy apparatus in cephalopods (see Kröger 2000; Keupp 2012; Hoffmann and Keupp 2015; De Baets et al. 2015; Lemanis et al. 2016b). Syncological factors can be reconstructed by the recognition of parasite infections or the presence of epizoa which in turn helped to reconstruct potential habitats and life habits. Lethal or sublethal injuries also add information on predator-prey interactions (e.g., Kauffman and Kesling 1960; Richter 2009). Recently, Keupp (2012) provided a detailed overview on palaeopathological belemnite rostra and introduced forma aegra-types for recurring kinds of abnormalities following the scheme developed for ammonoids by Hölder (1956). It should be noted that forma aegra-types do not refer to taxonomic entities but are a type of open nomenclature for the classification of pathologies. For fossil coleoid cephalopods, including belemnites, three categories of palaeopathologies can be distinguished based on their causes: (i) regeneration of injuries including inflammatory infection often caused by an unsuccessful predatory attack, (ii) prod traces due to collisions, (iii) parasite infection.

Most malformations of belemnite rostra resulted from mechanical injuries, often caused by failed predation attempts (Schwegler 1939), and less commonly from parasite infestations. Abel (1916), Daqué (1921), Tasnadi-Kubasca (1962), and Richter (1993) argued that rostra broke due to mechanical stress induced during active digging in the sediment with the rostrum. Due to the likely nektonic lifestyle of belemnites and the counterweight function of the rostrum (Monks et al. 1996; Jenny et al. 2019) that allows a horizontal swimming position, injuries due to digging are highly unlikely.

Application of non-invasive imaging methods such as computed-tomography (CT) or magnetic resonance imaging (MRI) have become a standard technique in palaeontology (e.g., Hoffmann et al. 2014; Lemanis et al. 2015, 2016, b; Rita et al. 2018). Mietchen et al. (2005) applied MRI to pathological belemnites under the assumption that CT-analysis of the dense low-Mg calcite of the rostra would have resulted in a poor image quality (low signal-to-noise ratio). Due to technical specifications the maximum spatial resolution of the MR-images was approximately around 100 µm, and scanning process took 18–93 hours (Mietchen et al. 2005; Ziegler et al. 2018).

Here, we demonstrate that nano-CT scanning of pathological belemnite rostra provide data with an excellent resolution, allowing a detailed description of internal features including malformations. High resolution and good signal to noise ratios in the resulting CT-images are important for the successful study of pathological belemnite rostra because of the continuous deposition of concentric growth increments. That mode of growth resulted in a successive attenuation of the primary morphology of the injury and the resulting symptom due to the deposition of post-traumatic growth increments. Based on CT-data, we provide short descriptions of the different types of palaeopathologies and discuss their potential causes. Furthermore, we demonstrate additional

applications such as the recognition of a heterogeneous or homogenous composition of belemnite rostra due to diagenesis, sedimentary fill, structures of the rostrum surface, and internal structures of the phragmocone such as septal spacing and the position of the siphuncle.

Institutional abbreviations.—CASP, Cambridge Arctic Shelf Programme, UK; DK (Danekrae) and GM, Natural History Museum of Denmark (Geological Museum), Copenhagen, Denmark; MGUH, Geological Museum of Copenhagen; Denmark; PIMUZ, Paläontologisches Institut und Museum Universität Zürich; Switzerland; RUB-Pal, Ruhr-Universität Bochum, Paläontologie; Germany; RE, Stiftung Ruhr Museum Essen (formerly: Ruhrlandmuseum Essen), Germany; SNSB-BSPG, Staatliche Naturwissenschaftliche Sammlungen Bayerns, Bayerische Staatssammlung für Paläontologie und Geologie, München, Germany.

Other abbreviations.—CT, computed-tomography; MRI, magnetic resonance imaging.

Material and methods

A total of 18 pathological belemnite rostra from Lower Jurassic (Toarcian) to Upper Cretaceous (Campanian) deposits, were CT-scanned. The material can be attributed to the following genera (in alphabetical order, number of studied specimens in parenthesis): ?*Acrocoelites* sp. (1), *Belemnellocamax* spp. (4), *Belemnitella* sp. (2), *Duvalia emERICI* (1), *Goniocamax* sp. (1), *Goniot euthis* spp. (5), *Hibolithes jaculoides* (2), *Neoclavibelus subclavatus* (1), and *Pseudobelus* sp. (1).

Some of the malformed rostra were described earlier by Mietchen et al. (2005), Keupp (2012), Weissmüller (2017), Hoffmann and Weissmüller (2018), and Thomel-Piccollier (2018). Only for *Goniocamax* sp. (DK 959; see Bonde et al. 2008) CT-data have already been published (Hoffmann et al. 2018), otherwise we present new findings. For additional data of the specimens or CT-data related information see SOM, Supplementary Online Material available at http://app.pan.pl/SOM/app65-Hoffmann_etal_SOM.pdf.

All specimens were scanned with the micro-computed-tomograph (micro-CT) nanotom m (GE Phoenix, Wunstorf, Germany) at the iWP company in Neuss (Germany) by Hendrik Wesendonk. Some specimens were scanned twice, including an overview and a close-up scan of the abnormally formed area to guarantee the best image quality. The cone beam reconstruction was performed using the GE datoslx 2 reconstruction software. For the visualisation, we used VG Studio Max 3.0 (Volumegraphics, Heidelberg). Acquired CT-data were used to generate all grey scale images used herein. Variations of grey scale values indicate either different dimensions of a chemically homogenous structure, or differences in the chemical composition or density, or a combination of both. Areas with light grey scale values

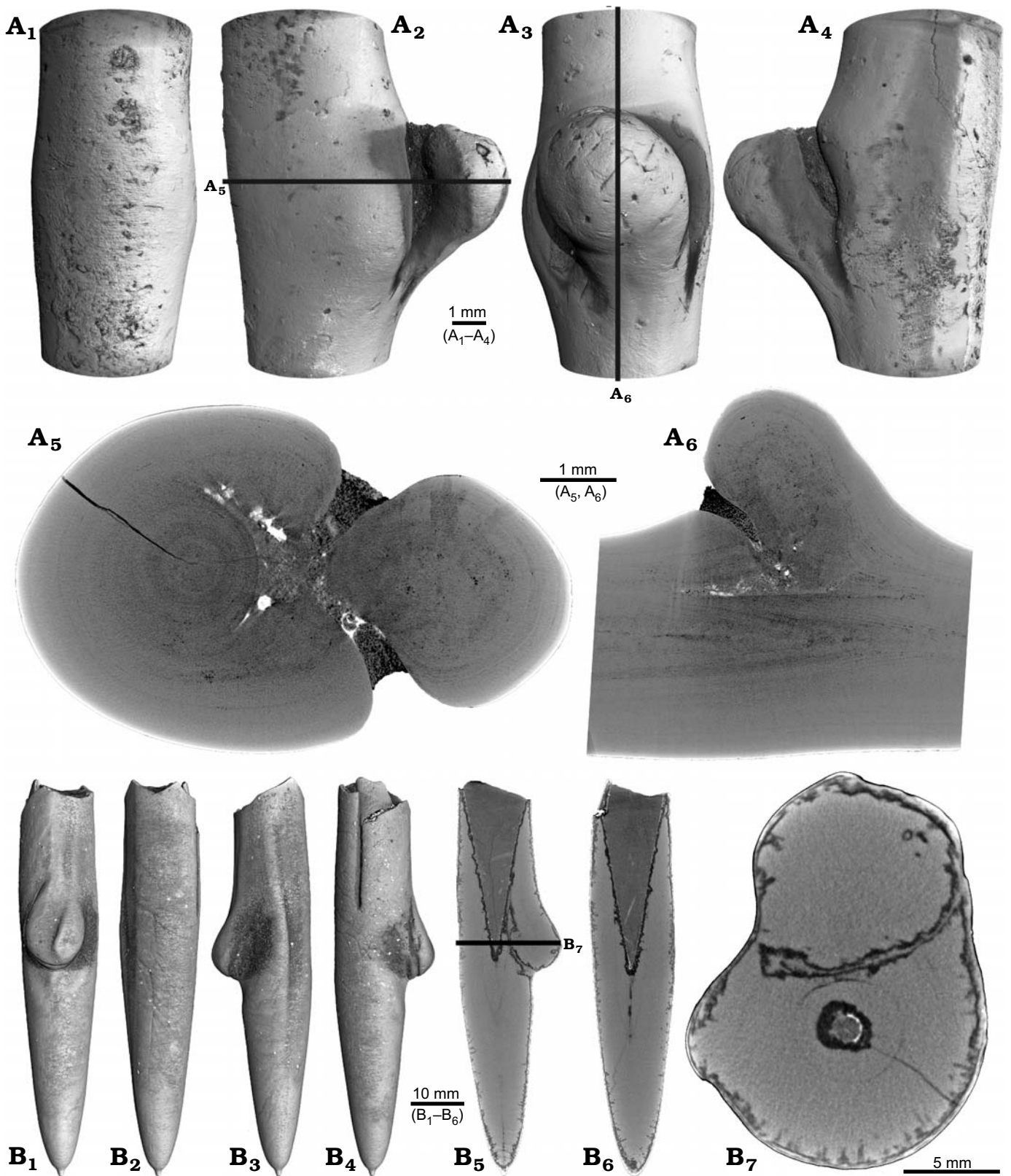


Fig. 3. **A.** Rostrum of belemnite *Neoclavibelus subclavatus* (Voltz, 1830), SNSB-BSPG-83264, Toarcian, Mistelgau (SW-Germany) with forma aegra bullata (coll. H. Keupp). Surface images showing the bump-shaped irregular rostrum growth (A₁–A₄); longitudinal sections showing presence of sediment (diffuse grey) and pyrite (white) within the rostrum, and increasing irregular growth increments (A₅, A₆). **B.** Rostrum of belemnite *Belemnitella* sp., RE 551.763.333 A 5238, Late Cretaceous, NW-Germany with forma aegra bullata (coll. Baschin). Surface images showing the bump-shaped irregular rostrum growth and imprints of an organic network on the rostrum surface in dorsolateral (B₁, B₂) and ventrolateral (B₃, B₄) views; longitudinal sections (B₅, B₆), and cross section (B₇). B₅–B₇ showing silification (black) along the rostrum surface but also along the malformed area.

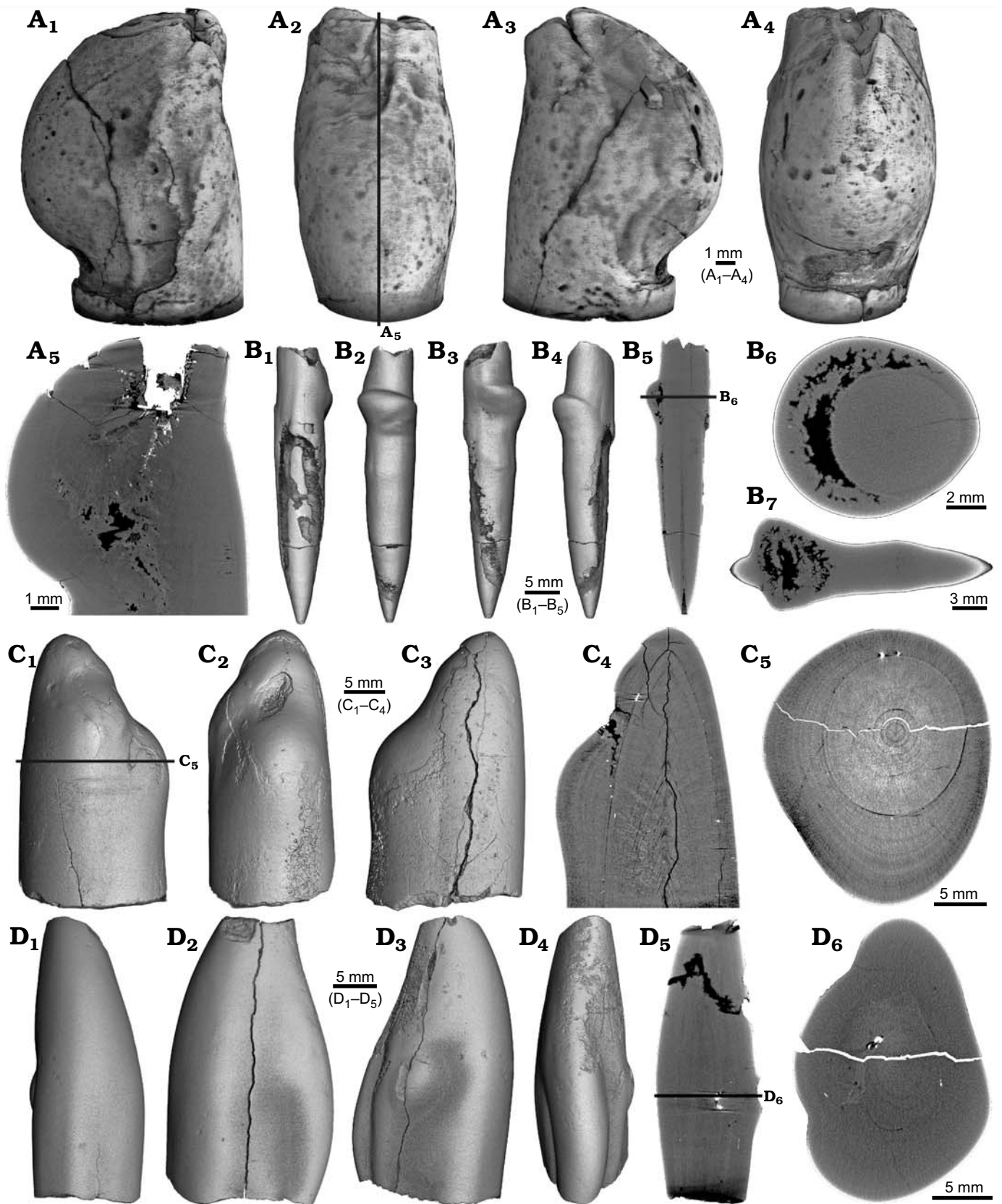


Fig. 4. **A.** Rostrum of belemnite cf. *Hibolites jaculoides* Swinnerton, 1937, SNSB-BSPG-83251, Hauterivian, Heligoland (N-Germany) with forma aegra bullata (coll. H. Keupp). Surface images showing the bump-shaped irregular rostrum growth, in lateral (A₁), dorsal (A₂), lateral (A₃), and ventral (A₄) views. Longitudinal section showing open pore space partially filled with carbonate cements (A₅). **B.** Rostrum of belemnite *Goniocamax* sp., MGUH 32024, Santonian, Bavnodde (Denmark) with forma aegra bullata (coll. J. Ansorge). Surface images of the rostrum showing the bump-shaped irregular →

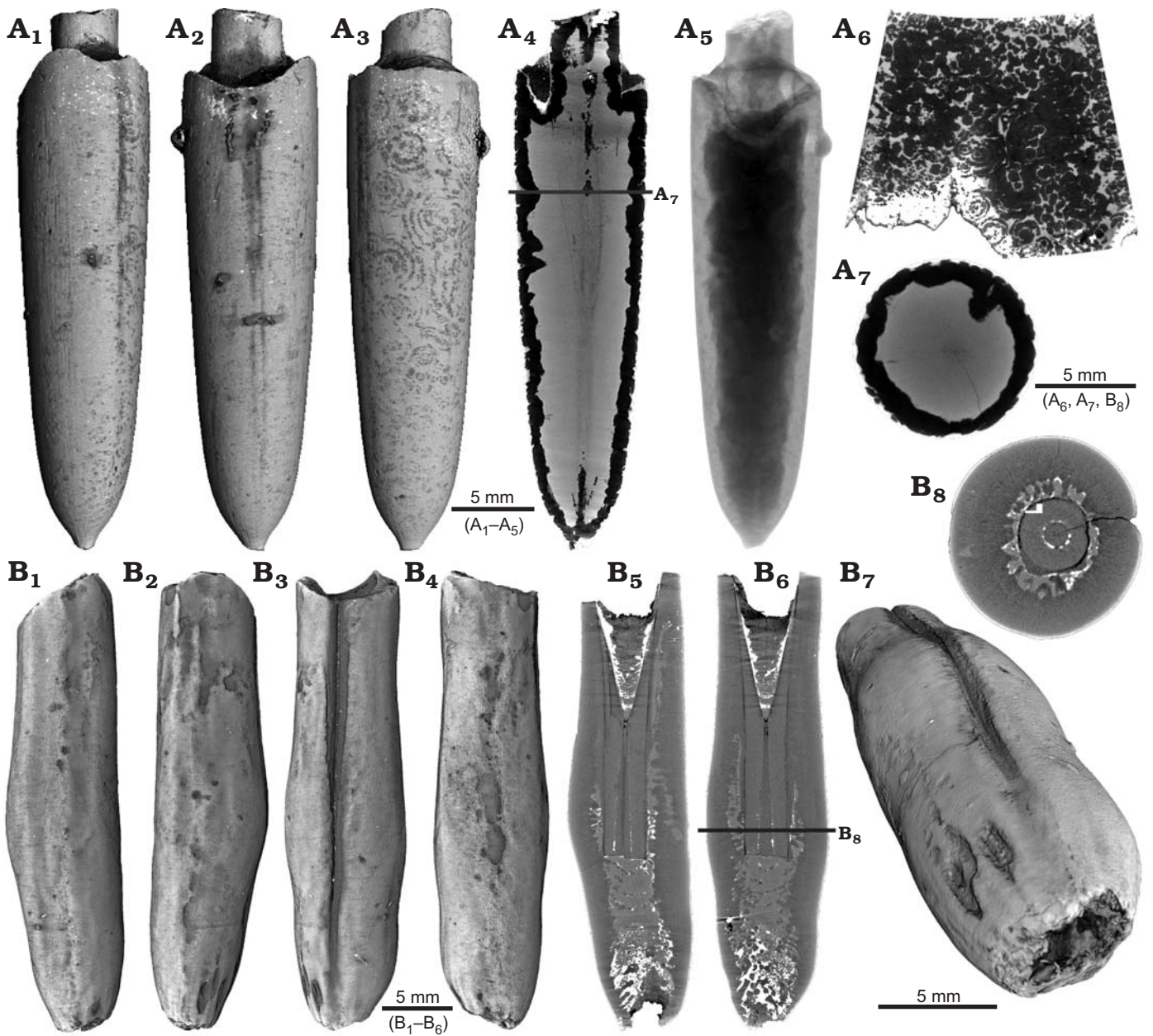


Fig. 5. **A.** Rostrum of belemnite *Gonioteuthis* sp., RUB-Pal 11301, Campanian, Höver (NW-Germany) with forma aegra clavata (coll. L. Kaecke). Surface images showing no irregularities except for silification rings (A₁–A₃). Longitudinal section showing a homogenous internal rostrum with a dark layer along its outer margin (silica) (A₄). Volume rendering image shows a darker centre due to the maximum thickness of the structure but no additional features (A₅). Detail of the rostrum surface showing silification rings (A₆). Cross section with a homogeneous centre and a dark margin (A₇). **B.** Rostrum of belemnite *Hibolites jaculoides* Swinnerton, 1937, RUB-Pal 11303, Hauterivian, Resse (NW-Germany) with forma aegra clavata (coll. U. Frerichs). Surface images showing the overall irregular rostrum morphology and the blunt and hollow apex in lateral (B₁, B₂), ventral (B₃), and dorsal (B₄), apical (B₇) views. Longitudinal sections (central, subcentral) showing the broken juvenile rostrum, parts of the preserved phragmocone, and notable the lack of the apical line after the injury took place, note the irregular outline of the hollow central canal (B₅, B₆). Cross section with the juvenile rostrum, and subsequently deposited homogeneous material, white areas indicate the presence of pyrite (B₈).

rostrum growth (B₁–B₄). Longitudinal section with growth increments, apical line, and the bump-like structure with pore space (black) (B₅). Cross section through the malformed area showing the pore space partially filled with carbonate cement (B₆). Marginal section through the malformed area (B₇). **C.** Undetermined belemnite, CASP K9068, Greenland, Early Cretaceous with forma aegra bullata. Surface images of the rostrum showing the irregular rostrum area (C₁–C₃). Longitudinal section showing growth increments, apical line and a distinct growth increment at which the malformation starts (C₄). Cross section that shows the distinct growth increment, and a horizontal fracture (white), as well as grains of pyrite (white) (C₅). **D.** Rostrum of belemnite *Duvalia emerici* (Raspail, 1829), RUB-Pal 22170, Late Valanginian, Laborel (France) with forma aegra bullata. Surface images of the rostrum showing the irregular rostrum area (half-pearl shaped), in ventral (D₁), lateral (D₂, D₃), and dorsal (D₄) views. Longitudinal section through the malformed area (D₅). Cross section, both section reveal that the structure is massive, i.e., not a blister pearl (D₆).

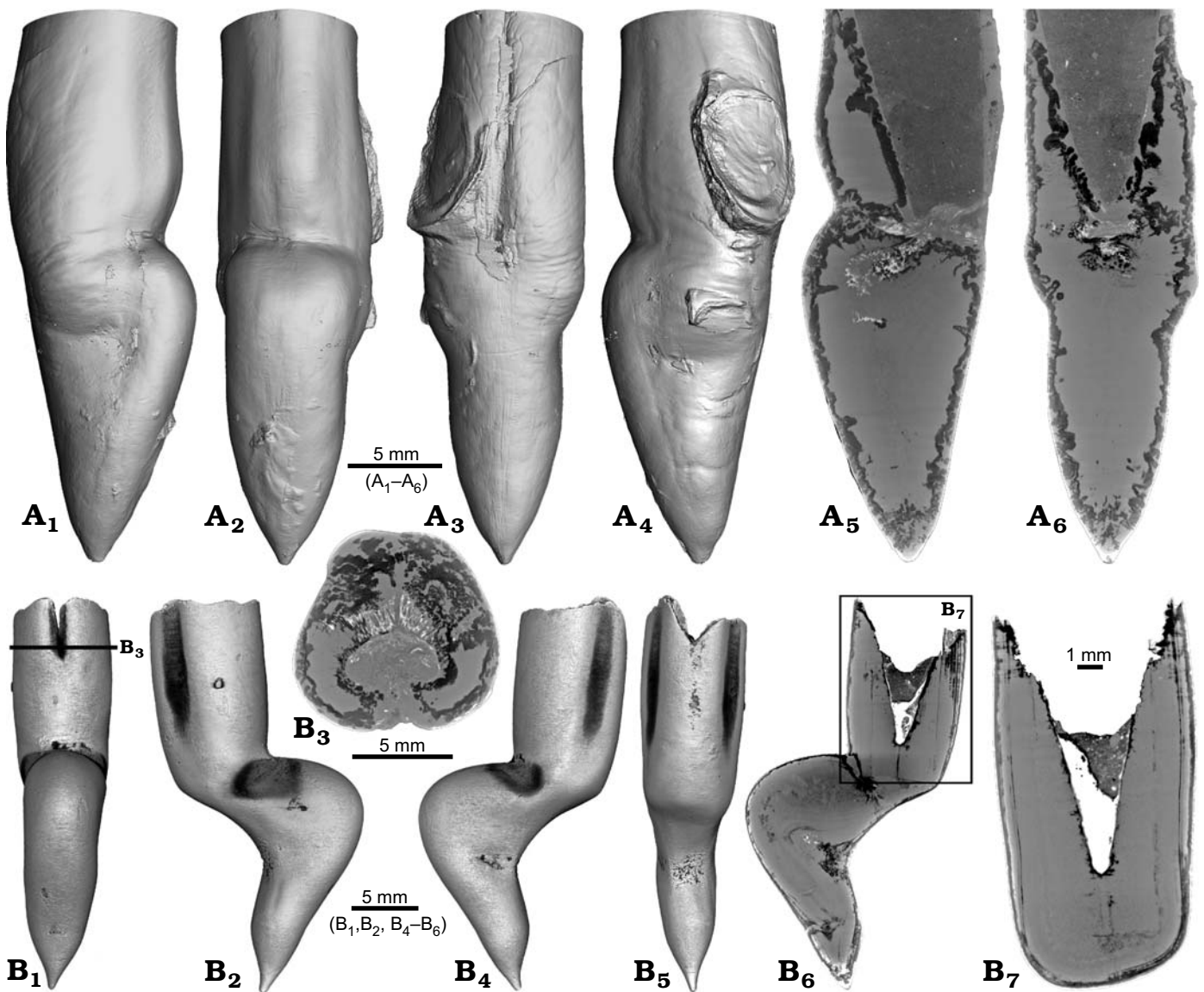


Fig. 6. Rostra of belemnite *Gonioteuthis* spp. **A.** RUB-Pal 11302, Campanian, Höver (NW-Germany) with forma aegra angulata (coll. U Frerichs). Surface images showing the knee-like morphology of the rostrum, and the attachment-base of an oyster, in lateral (A_1 , A_4), dorsal (A_2), and ventral (A_4) views; note the weak furrows in A_3 . Median sections perpendicular to each other showing silicified areas (darker) and the broken phragmocone now filled with sediment, no additional internal feature visible (A_5 , A_6). **B.** SNSB-BSPG-83246, Campanian, Höver (NW-Germany) with forma aegra angulata (coll. H. Keupp, leg. C. Spaeth). Surface images showing the knee-like morphology of the rostrum, in ventral (B_1), lateral (B_2 , B_4), and dorsal (B_5) views. Cross section (B_3). Median sections showing silicified areas specifically at places heavily bent (darker) (B_6 , B_7); see also A_5 , A_6 for the same phenomenon. Black box indicates close up in B_7 , showing the broken juvenile rostrum with growth increment (forma aegra clavata), and the phragmocone partially filled with pyrite (white).

represent the dense calcite of the belemnite rostrum, while darker to black areas are related to structures with a very low density such as gas-filled pores. Presented images are surface renderings, volume renderings, and orthoslices.

Results

We describe various pathologies encountered according to their morphological expressions including two-tipped specimens, blisters and pearls, broken rostra, which healed straight, rostra with a kink or bent rostra (Figs. 1–9). Differences in grey scale values in the images suggest different

materials such as calcite, silica, pyrite, or sediment. The growth increments of the rostrum, for example, are visible in CT-images due to the varying amount of organic matter, which has significant lower absorption properties compared to pure calcite. This implies that organic-rich growth increments are darker compared to those composed of pure calcite.

One *?Acrocoelites* sp. (PIMUZ 37346) and one *Gonioteuthis* sp. (RUB-Pal 11264) rostrum are characterized by two divergent apices (Figs. 1, 2). In both specimens one apex represents the continuation of the original rostrum axis and bears radial striation on its outer surface (*?Acrocoelites* sp., Fig. 1A, B_1 – B_4 ; *Gonioteuthis* sp., Fig. 2A $_1$ –A $_5$). The second

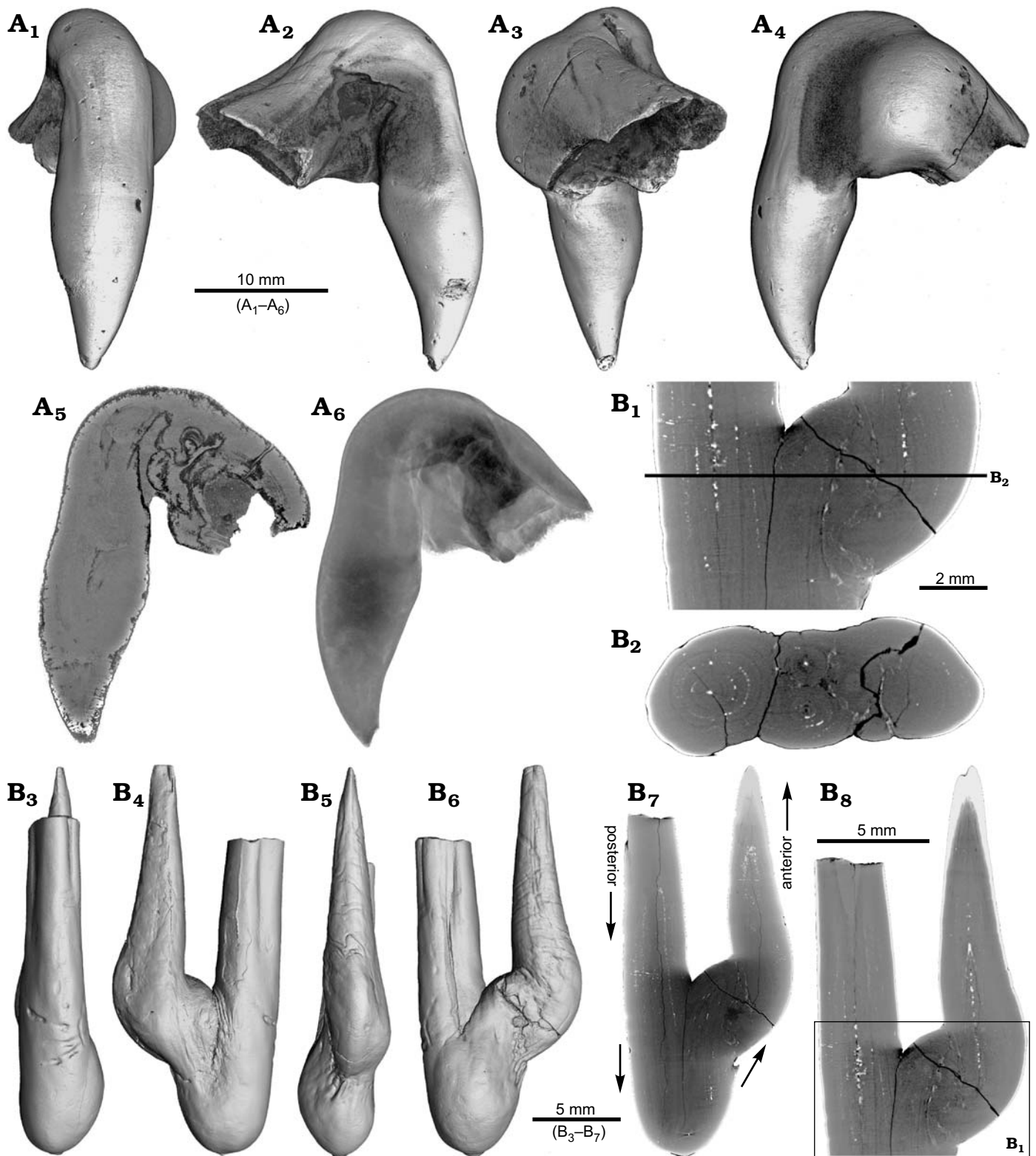


Fig. 7. **A.** Rostrum of belemnite *Gonioteuthis* sp., SNSB-BSPG-83370, Campanian, Höver (NW-Germany) with forma *aegra hamata* (coll. H. Keupp, leg. C. Spaeth). Surface images showing the knee-like strongly bent and irregular morphology of the rostrum (A₁–A₄). Median section showing the irregular internal silification of the rostrum indicating poorly mineralized areas, growth and apical line partially visible (A₅). Volume rendering image with the darkest areas represented by the thickest or densest areas (A₆). **B.** Rostrum of belemnite *Pseudobelus* sp., RUB-Pal 3196, Valanginian, Barret-Meouge (France) with forma *aegra hamata* (coll. M.-C. Picollier). Surface images showing the strongly bent and irregular morphology of the rostrum with the apex growth in anterior direction (B₃–B₆). Median section overview and close up showing growth increments and the presence of pyrite along the apical line (white) (B₁, B₇, B₈). Cross section showing four growth center representing a temporal sequence (B₂).

apex of *?Acrocoelites* sp. bears one strong dorsal furrow. Superficially, the arrangement of the *?Acrocoelites* sp. apices resembles a crustacean claw. Unfortunately, the CT-data did not reveal the course of growth increments or other internal structures, which suggests an irregular formation of the skeletal calcite (Fig. 1B₅).

The continuation of the normal rostrum growth in the *Goniot euthis* sp. is supported by the presence of the apical line and growth increments (Fig. 2B₁). The rostrum surface of this *Goniot euthis* sp. partially shows dissolution features or poorly mineralized layers exposing triangular structures (Fig. 2A₁–A₃, A₆). Some of these features suggest the presence of meandering trace fossils (Fig. 2A₅). Both apices were partially hollow and subsequently filled with sediment (Fig. 2B, C₁, C₂). Development of the two apices is reflected in the image series in Fig. 2C based on virtual cross sections. Areas darker than the calcitic parts of the rostrum and mostly restricted to the rostrum surface indicate the presence of silica.

One *Neoclavibelus subclavatus* (SNSB-BSPG-83264) and one *Belemnitella* sp. (RE 551.763.333. A 5238) rostrum each show a bump-like structure (Fig. 3). Virtual cross sections of the *N. subclavatus* rostrum reveal the presence of sediment inside the rostrum. This debris was subsequently overgrown by calcite precipitated by the belemnite, causing the malformation (Fig. 3A₅, A₆). The longitudinal section shows that the contaminant covers parts of the juvenile rostrum, thereby causing a deviation in growth increment orientation (Fig. 3A₆). White areas suggest the presence of pyrite, which completely absorbs the X-rays. The bump-like structure in the *Belemnitella* sp. rostrum (Fig. 3B₁, B₃–B₅) was probably caused by a similar process. In this case, the foreign material caused the bending of dorsolateral depressions covering the rostrum surface (Fig. 3B₃). Darker areas along the margin of the rostrum suggest the presence of silica (Fig. 3B₅–B₇). For both species, we also provide high-resolution CT-images (*Hibolithes jaculoides*, Fig. 4A; *Goniot camax* sp., Fig. 4B). A large part of the *Goniot camax* sp. rostrum shows signs of exfoliation. Our CT-based examination of the area where outer rostral layers thin out reveals, that sediment was deposited between distinct growth increments of the belemnite rostrum. Both specimens show hollow areas, partially filled with carbonate crystals, within the rostrum forming blisters. The *Goniot camax* sp. blister is elongated with a spiral morphology. The sediment filled blister contrasts with the massive bump-like structures of another two specimens (undetermined specimen (CASP K9068), Fig. 4C; *Duvalia emerici*, Fig. 4D). The undetermined rostrum shows a distinctive layer from which the growth perturbation starts (Fig. 4C₄, C₅) in longitudinal- and cross section. This structure resembles the phenomenon described for *N. subclavatus*

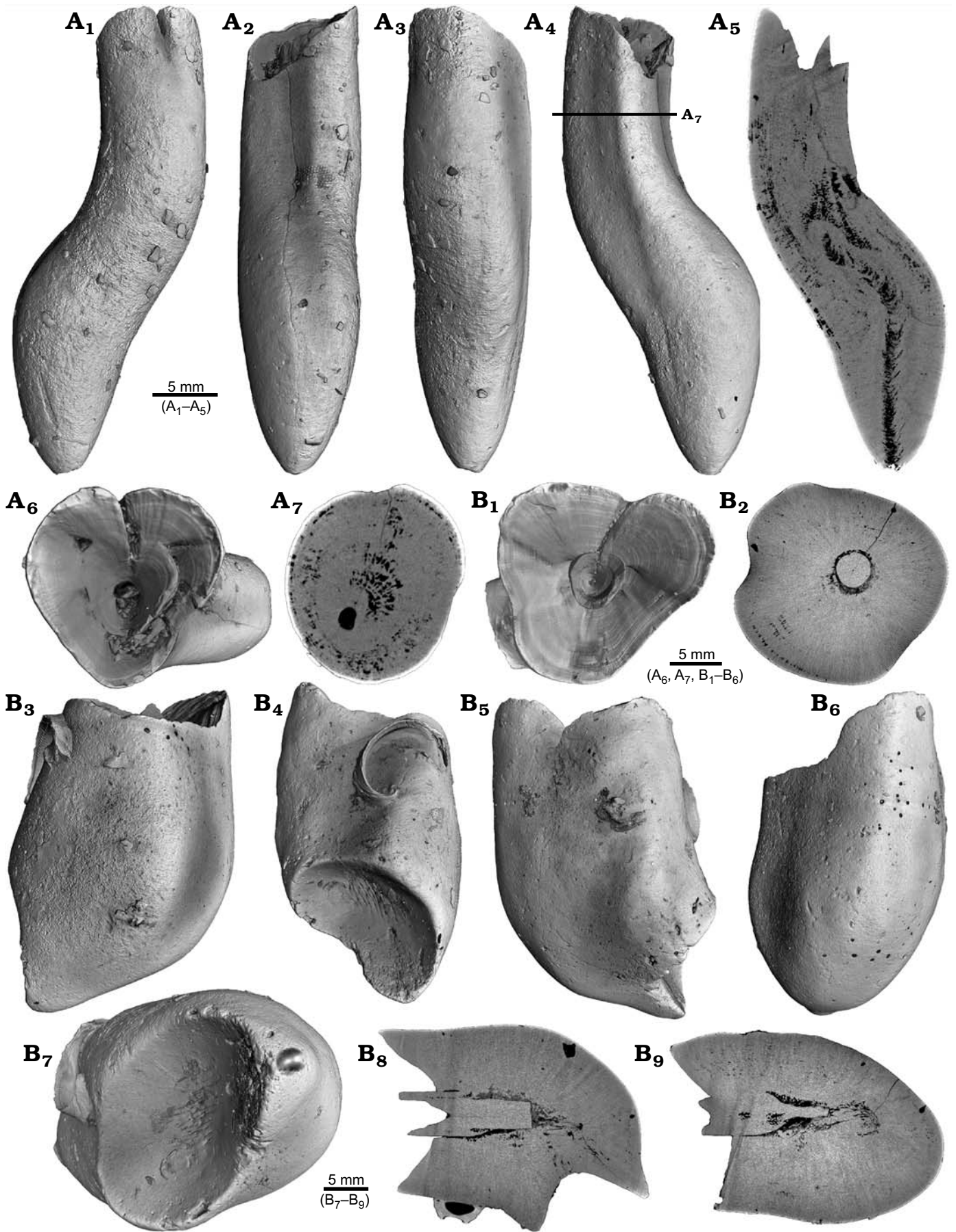
and *Belemnitella* sp. For *D. emerici*, no such perturbation has been identified (Fig. 4D₅, D₆).

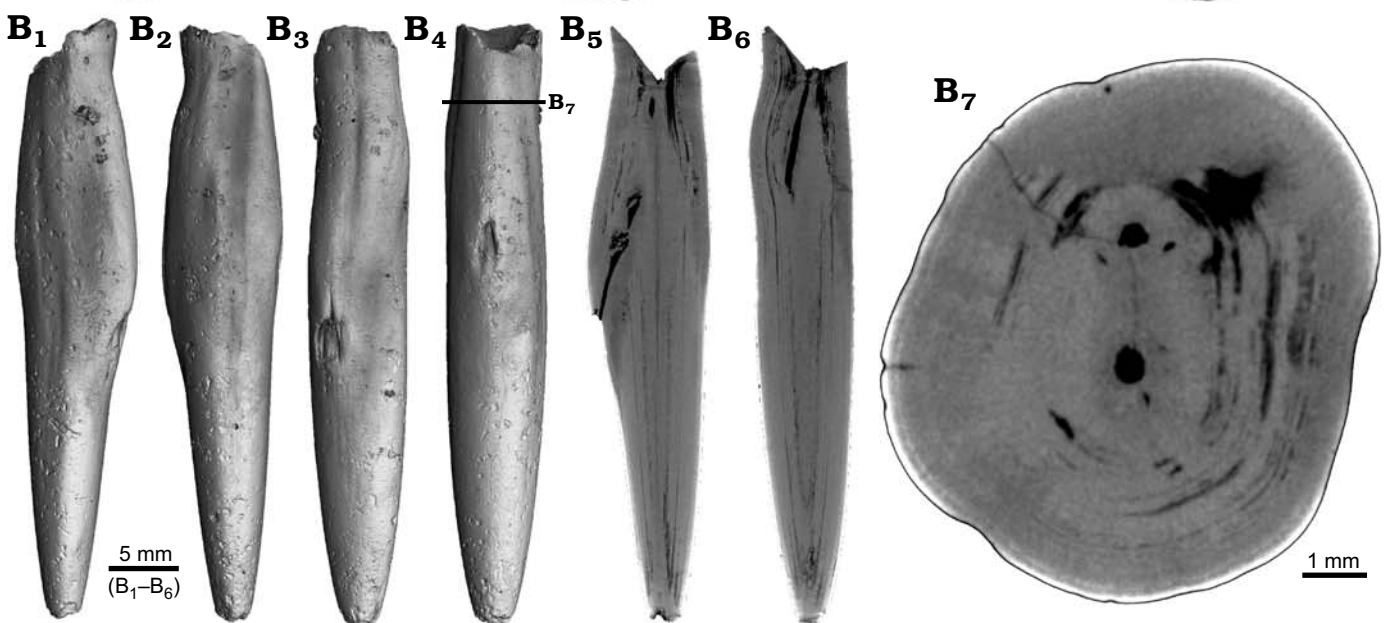
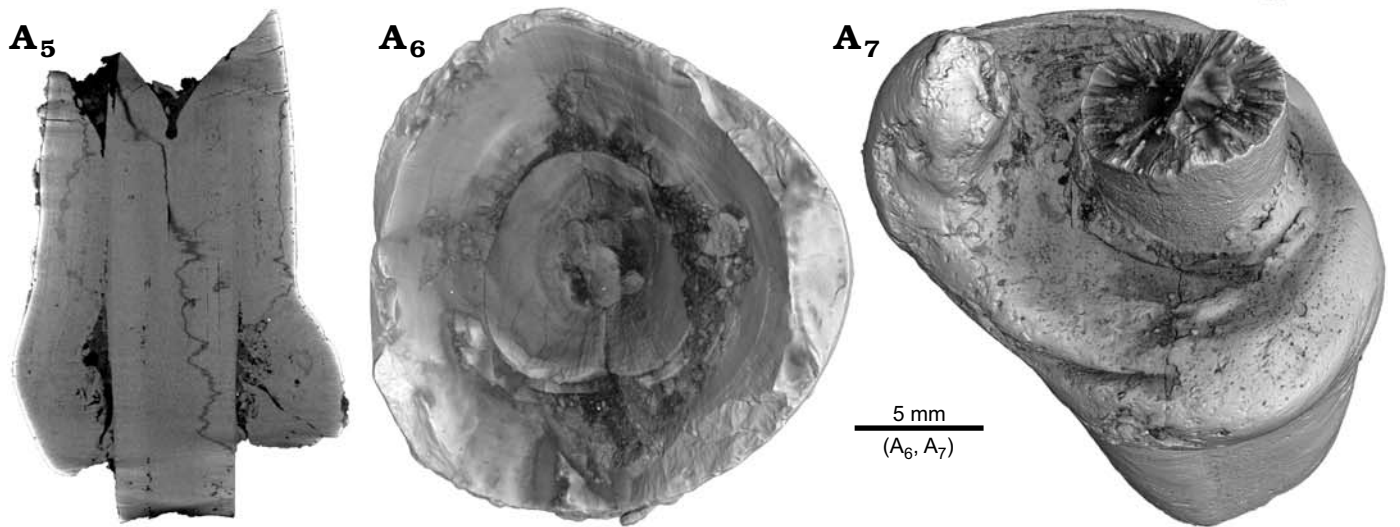
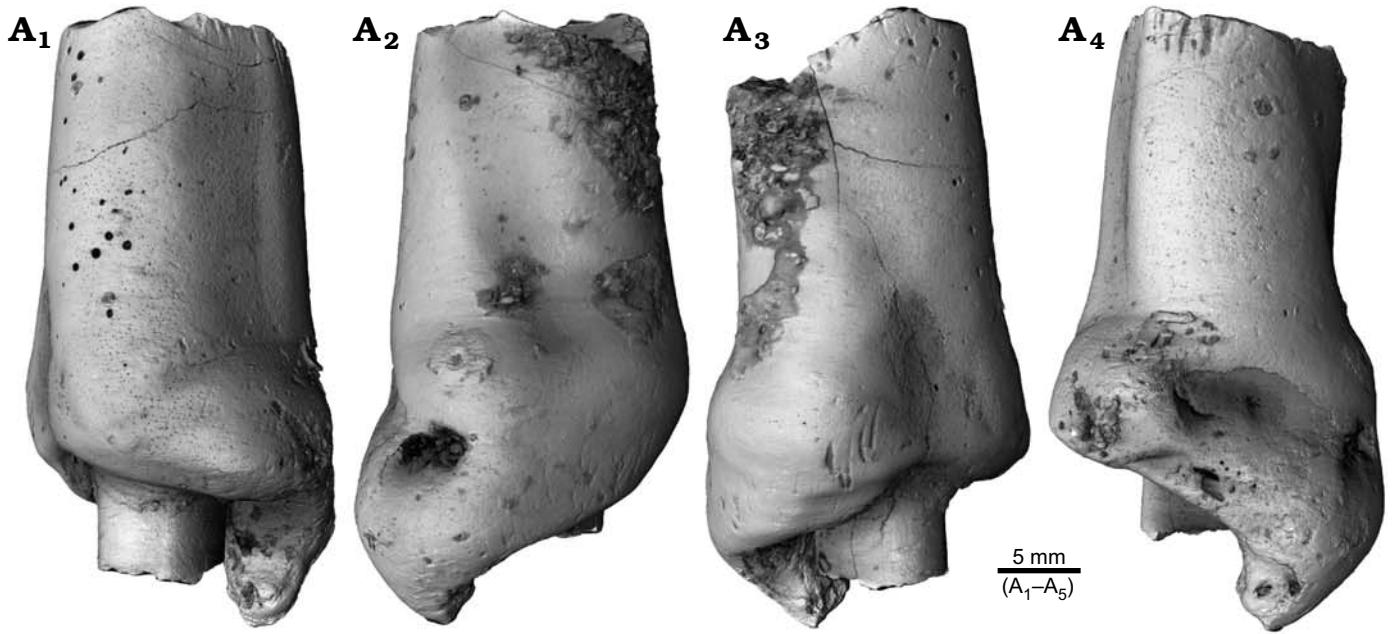
One belemnite assigned to *Goniot euthis* sp. (RUB-Pal 11301) and one assigned to *Hibolithes* sp. (RUB-Pal 11303) have fractured rostra (Fig. 5). Due to strong silification, the results from the CT-scans remain inconclusive for the *Goniot euthis* sp. rostrum (Fig. 5A). The apical line appears to form a continuous line without the formation of a blunt rostrum (Fig. 5A₄). Parts of the rostrum increments seem to be poorly mineralized, causing parts of the juvenile rostrum to stick out where normally the alveolus is situated. This example demonstrates the potential of the CT technique to better understand the mineralogical composition of belemnite rostra. In our case silification rings (Fig. 5A₃, A₆) correspond to darker areas in virtual section images (Fig. 5A₄, A₇). Virtual sections of the *H. jaculoides* rostrum reveal a broken juvenile rostrum with the apex missing (Fig. 5B₅, B₆). The fracture was overgrown by irregularly formed rostrum material. While the outer layers show regularly formed growth increments, the internal part appears to be chaotic without forming an apical line. This irregular growth results in a rostrum morphology comparable to the genus *Produvalia* (Fig. 5B₇).

Two specimens of *Goniot euthis* spp. display a marked distortion of the rostrum (Fig. 6). Both, the rostrum and the phragmocone were affected in one specimen, post mortem overgrown by an oyster (Fig. 6A₂–A₄). In this case parts of the juvenile rostrum are not preserved (RUB-Pal 11302; Fig. 6A₅, A₆). The rostrum surface shows faint radial striae (Fig. 6A₃). The second specimen (SNSB-BSPG-83246) yields an intact phragmocone but parts of the juvenile rostrum broke off (Fig. 6B₆, B₇). The phragmocone is partially filled with pyrite (white area) and sediment (irregular greyish). Due to partial silification, the growth increments are well visible. Areas with strong bending are silicified, and the rostrum surface is rough due to dissolution, poor mineralization, or both (Fig. 6B₅, B₆; compare with Fig. 2A). Although strongly bent, the rostrum shows growth increments and an apical line.

One rostrum each of *Goniot euthis* sp. and *Pseudobelus* sp. are strongly distorted resulting in a change of growth direction (Fig. 7). The specimen of *Goniot euthis* sp. (SNSB-BSPG-83370) deviates from the normal (= straight) growth direction by about 90° with its apex pointing slightly towards the alveolus (Fig. 7A). A small part of the phragmocone, now filled with sediment, is preserved and the rostrum is heavily silicified. A few growth increments and a faint trace of the apical line are visible (Fig. 7A₅). The rostrum of *Pseudobelus* sp. (RUB-Pal 3196) shows the strongest deformation reported here. CT-data suggest three traumatic events resulting in fractures and finally a reversion of the growth direction

Fig. 8. Rostra of belemnite *Belemnellocamax* spp., Campanian, Ivo Klack (Sweden). **A.** GM 04.1918, forma aegra angulata. Surface images showing the knee-like morphology of the rostrum (A₁–A₄). Longitudinal section showing the porous apical area (black) (A₅). Alveolar region (A₆). Cross section showing pore space within the rostrum (black) (A₇). **B.** GM 02.1918, forma aegra clavata. Alveolar region (B₁). Cross section with the juvenile rostrum in its centre (B₂). Rostrum surface of the short, stout rostrum with a blunt apex and a concave impression (?dissolution feature), in lateral (B₃–B₆) and apical (B₇) views. Central and subcentral longitudinal section with the juvenile rostrum and the surrounding porous area (B₈, B₉). →





towards the head of the animal. Growth increments and apical line are, however, well visible in the longitudinal section (Fig. 7B₁, B₇, B₈). The cross-section image (Fig. 7B₂, along the black line in Fig. 7B₁) shows four growth zones representing a temporal sequence implying that the rostrum broke during four successive and independent events.

Four malformed specimens of *Belemnellocamax* sp. with fractured rostra show weak to strong reactions that occurred during the healing process (Fig. 8, 9). One specimen (GM 04.1918) is a knee-like bent rostrum (Fig. 8A₁–A₄) with a spongy, highly porous internal structure (Fig. 8A₅, A₇). A second specimen (GM 02.1918) has a short rostrum with a blunt apex due to a spherical depression (Fig. 8B₃–B₇). The virtual section reveals a broken juvenile rostrum associated with a porous area surrounding it (Fig. 8B₈, B₉). The third specimen (GM 01.1918) also has a broken juvenile septum, which extended beyond growth increments of older parts of the rostrum (Fig. 9A₁–A₅, A₇). Subsequently formed growth increments never covered the juvenile rostrum entirely, forming a callus-like structure. Parts of the alveolar region are preserved allowing for a correct orientation of the rostrum (Fig. 9A₅). Specimen four (GM 03.1918) shows a slightly irregular rostrum morphology with curved depressions and a small hole on the rostrum surface. Virtual longitudinal sections reveal that the hole at the surface is connected to a canal that appears to start in the central alveolar region (Fig. 9B₅, B₆, B₇). Growth increments, otherwise well visible, disappear around the canal.

Discussion

Like all coleoid cephalopods, belemnites formed their internal shell within the shell sac (Bandel and Boletzky 1979; Bandel 1982). Belemnite rostra were secreted by the muscular mantle that is fused above the shell mantle in endo-cochleate cephalopods (Bandel and Spaeth 1988). Growth increments are rhythmically added to the rostrum by simultaneous accretion on its surface. This mode of biomineralization is comparable to the formation of the cuttlebone sheath of sepiids including the spine (Bandel and Spaeth 1988; Fuchs 2012; Checa et al. 2015), which contains high amounts of organic material. The rostrum is composed of radiaxial calcite fibres that cross the concentric growth increments (Richter et al. 2011; Hoffmann et al. 2016; Stevens et al. 2017; Hoffmann and Stevens 2019).

The recent application of non-invasive imaging methods other than MRI to belemnite rostra, such as synchrotron radiation based micro-CT by Hoffmann et al. (2016), revealed

the presence of a new rostral ultrastructure, suggesting a composition of two distinct calcite phases. Micro-CT was used by Wisshak et al. (2017) to describe bioerosion features (trace fossils), which are often found on belemnite rostra. Rita et al. (2018) used micro-CT-data to determine rostrum volumes to reconstruct temporal changes in belemnite size. The description of a variety of pathological phenomena highlights the advantage of the higher spatial resolution and suitable contrast properties accessible by CT-derived volume data to explore the three-dimensional nature of pathological specimens. The following forma aegra-categories (= malformation categories) were used to group the various types of malformation as outlined by Keupp (2012).

Linking observed malformations with the forma aegra-types.

Apex malformation (= forma aegra saepia; Figs. 1, 2).—This malformation describes a duplication or multiplication (up to five apices known so far) of the rostrum apex (e.g., Finzel 1963; Schmid 1963; Miertzsch 1964; Keupp 2002, 2012; Mietchen et al. 2005; Hoffmann and Weissmüller 2018). Keupp (2012) argued that due to traumatic events (mechanical injuries) or the activity of parasites parts of the apex forming mantle epithelium were separated into locally independent secretion centres that formed several apices. Here, we report forma aegra saepia for one specimen of *?Acrocoelites* sp. and *Gonioteuthis* sp. each.

Blister malformation (= forma aegra bullata; Figs. 3, 4).—This malformation includes blister thickenings of the rostrum often enclosing a hollow space, which may indicate the earlier presence of endoparasites. The locally proliferating mineralization of the rostrum can in rare cases lead to the formation of a second rostrum paralleling the primary rostrum (Keupp 2012: fig. 405; Dietrich et al. 2013; Frerichs 2015; Hoffmann et al. 2018). Here, we report forma aegra bullata for one specimen of *Neoclavibelus subclavatus*, *Belemnitella* sp., *Hibolithes jaculoides*, *Goniocamax* sp., an undetermined belemnite, and *Duvalia emerici* each.

Blunt rostra (= forma aegra clavata; Figs. 5, 8B, 9A).—This malformation contains more or less club-shaped rostra that are thicker and shorter compared to normal specimens. They are the result of broken juvenile rostra. Depending on the timing and severity of the fracture, slightly to heavily deformed rostra result. Often, the earliest parts of the phragmocone including the initial chamber are affected (Keupp 2012: fig. 381, top). Extreme shortenings of the rostrum results in a droplet-shaped morphology (Kabanov 1967; Keupp 2012). Here, we report forma aegra clavata for one specimen of

← Fig. 9. Rostra of belemnite *Belemnellocamax* spp. **A.** GM 01.1918, Campanian, Ivo Klack (Sweden) with forma aegra clavata. Surface images showing the collar-like structure and parts of the juvenile rostrum (A₁–A₄). Longitudinal section (A₅) showing the sediment filled phragmocone with the protoconch, the Klähn'sche plane (Klähn 1925), the juvenile rostrum, and the material added after the traumatic event forming a collar-like structure but not covering the juvenile rostrum completely. Alveolar region (A₆). Opposite side with the juvenile rostrum sticking out (A₇). **B.** GM 03.1918, Campanian, Ugnsmunnarna (Sweden) with forma aegra collata. Irregular outline morphology of the rostrum (B₁–B₄). Longitudinal section to show the canal, growth increments (B₅, B₆). Cross section through the apical line and the canal (B₇).

Goniot euthis sp., one specimen of *H. jaculoides*, and two *Belemnello camax* sp. specimens.

Bent rostra (= forma aegra angulata; Figs. 6, 8A).—This malformation is characterized by multiple rostrum fractures. The dislocated rostrum fragments were covered by post-traumatic growth increments. Depending on the size and position of the fragments within the mantle sac, distortions of variable angles (within a plane or a screw-like arrangement of the fragments in different planes) resulted. Such fractures were described by several authors (e.g., Duval-Jouve 1841; Kabanov 1967; Doyle 1990; Kraus 2000; Keupp 2002, 2012; Mietchen et al. 2005; Hüne and Hüne 2008). This phenomenon includes specimens with fragments grown together sub-parallel to each other after the attack (see Moosleitner 2012; Keupp 2012: fig. 397). Here, we report forma aegra angulata for two specimens of *Goniot euthis* spp. and one specimen of *Belemnello camax* sp.

Hook-shaped rostra (= forma aegra hamata; Fig. 7).—Hook-shaped rostra, as reported by Blainville (1827), are often the result of rostrum fractures that occurred during early ontogeny. Parts of the broken rostrum become dislocated and post-traumatic growth is preferentially oriented towards one side of the rostrum resulting in a change of growth direction (Duval-Jouve 1841; Radwańska and Radwański 2004; Moosleitner 2006; Keupp 2012). In case the rostrum becomes significantly shorter, a form transitional between the forma aegra hamata and forma aegra clavata exists (Keupp 2012). A 180° reversal of the growth direction of the rostrum towards the head of the animal due to several fractures (Fig. 7B₃–B₈) is documented in this study for the first time. Here, we report forma aegra hamata for one specimen of *Goniot euthis* sp. and *Pseudobelus* sp. each.

Sceptre-shaped rostra (= forma aegra manca; Fig. 5A).—The mechanical injury of the mantle sac epithelium can lead to a partial lack of growth increments. This is related to the disabled function of the injured epithelium to secrete shell material. This symptom is often observed in the apical area of the rostrum causing an incomplete apex. In this case juvenile, pre-traumatic parts of the rostrum form the apex. A damage of the lateral epithelium is related to a thinning of the rostrum in the affected area and result in a sceptre-shaped rostrum (Keupp 2012). Here, we report forma aegra manca for one specimen of *Goniot euthis* sp.

Collar formation (= forma aegra collata; Fig. 9B).—This deformation describes flap-like outgrowths at the sub-apical rostrum area without visible injury. This symptom was reported from a variety of Jurassic and Cretaceous belemnites and possibly results from a parasitic infestation (Keupp 2012). This infestation caused the formation of a collar (from Latin, *colla*) that is regarded as an effluence channel and potentially indicates an inflammation of the mantle sac epithelium. Here, we report forma aegra collata for one specimen of *Belemnello camax* sp.

Parasitism in belemnites

Most studies about modern molluscan parasites deal with parasites of bivalves. Bivalves host a diverse group of parasites and disease-causing agents such as, e.g., viruses, prokaryotes, fungi, protists, parazoans, and metazoans (platyhelminths, annelids, molluscs, bryozoans, and arthropods) (see Lauckner 1983; Huntley and De Baets 2015 for extensive reviews). Most of the parasites belong to endoparasitic flukes (Trematoda, Digenea), which have also been observed in gastropods (Ruiz and Lindberg 1989; Ozanne and Harries 2002; Littlewood and Donovan 2003; Huntley and De Baets 2015). Larvae of digenean trematodes (Gymnophallidae) sometimes lead to the formation of blisters (Götting 1979; Ituarte et al. 2001; Cremona and Ituarte 2003) and have been found also in fossil bivalves dating back to the Triassic (Boucot and Poinar 2010). Blister formation, however, can have a variety of causes, some of which are not due to parasites (Kinne 1983). Identification of a specific parasite taxon, however, is hampered by the fact that parasites are typically small-bodied (submillimetre) and usually lack biomineralized hardparts.

In modern cephalopods, parasites are known from many species from all major oceans ranging from coastal, shelf, to oceanic and deep-sea species (Hochberg 1990; Pascual et al. 1996, 2007; López-González et al. 2000; Gestal et al. 2019). This is no surprise given that cephalopods are a key trophic element in marine ecosystems (Clarke 1996). Hochberg (1990) documented 200 species of endoparasites in cephalopods with macroparasites such as, e.g., nematodes, copepods, and isopods. These predominantly affect non-mineralized tissues such as the digestive tract and the gills. The infestation of mainly non-mineralized tissues limits the fossil preservation potential of parasite activity and the resulting host reaction.

For belemnites, most reported pathologies are due to survived predator attacks (e.g., forma aegra angulata), a few malformations are assigned to the activity of parasites like, forma aegra bullata, collata, and saepia. Although we can identify a parasite infection as the most likely trigger of these pathologies, attributing the deformations to a specific parasite taxon is difficult to impossible. While some parasites leave characteristic patterns on their host, this is not necessarily definitive evidence of their presence. Different parasites can leave similar traces and taxonomically distant parasites can inflict similar symptoms on their hosts because of convergence in the evolution of host-exploitation strategies (Poulin 2011; Leung 2017). Differential diagnosis for palaeopathological phenomena may lead to the conclusion that two or more alternative conditions remain as potential triggers (Buikstra et al. 2017; Hoffmann et al. 2018).

Conclusions

Our high-resolution CT-data represent an innovative and non-destructive way to analyse the internal structure of bel-

emnite rostra. CT-images revealed internal structures that allow the examination of a variety of pathological phenomena and to differentiate between different types of pathology. Most importantly, the CT-data allow to infer potential causes of these deformations (predator attack or parasite activity), therefore going beyond a classification of pathologies from the surface of a specimen alone. We thereby demonstrated the usefulness and feasibility of the application of non-invasive imaging methods to the field of palaeopathology. The data gained can be further used for the identification of various diagenetic alteration features in belemnite rostra. CT-data turned out to perform better than MRI-data in terms of spatial resolution and contrast.

Acknowledgements

We are grateful to Jens Bruns (Rotenburg, Germany), Udo Frerichs (Langenhagen, Germany), Sten Lennart Jakobsen (Natural History Museum Copenhagen, Denmark), Lutz Kaecke (Hannover, Germany), Alexander Nützel (SNSB-BSPG), Udo Scheer (formerly Stiftung Ruhr Museum, Essen, Germany), Simon Schneider (CASP), and Mathias Weissmüller (Berg, Germany) for supplying material. We acknowledge the constructive reviews by Helmut Keupp (Freie Universität Berlin, Germany), Oksana Dzyuba (Trofimuk Institute of Petroleum Geology and Geophysics, Siberian Branch of RAS, Novosibirsk, Russia), and Max Wisshak (Senckenberg am Meer, Marine Research Department, Wilhelmshaven, Germany).

References

- Abel, O. 1916. *Paläobiologie der Cephalopoden aus der Gruppe der Dibranchiaten*. 281 pp. Jena Gustav Fischer Verlag.
- Bandel, K. 1982. Morphologie und Bildung der frühontogenetischen Gehäuse bei conchiferen Mollusken. *Facies* 7: 1–198.
- Bandel, K. and Boletzky, S. von 1979. A comparative study of the structure, development and morphological relationships of chambered cephalopod shells. *The Veliger* 21: 313–354.
- Bandel, K. and Spaeth, C. 1988. Structural differences in the ontogeny of some Belemnite rostra. In: J. Wiedmann and J. Kullmann (eds.), *2nd International Cephalopod Symposium Cephalopods—Present and Past*, 247–271. Schweizerbart, Stuttgart.
- Bertling, M., Braddy, S.J., Bromley, R.G., Demathieu, G.R., Genise, J., Mikulas, R., Nielsen, J.K., Nielsen, K.S.S., Rindsberg, A.K., Schlirf, M., and Uchman, A. 2006. Names for trace fossils a uniform approach. *Lethaia* 39: 265–286.
- Blainville, M.H.D. 1827. *Mémoire sur les Belemnites considérées Zoologiquement et Géologiquement*. 136 pp. F.G. Levrault, Paris.
- Bonde, N., Larsen, S., Hald, N., and Jakobsen, S.L. 2008. *Danekrae, Danmarks bedste fossiler*. 224 pp. Gyldendal, København.
- Boucot, A.J. and Poinar, G.O. 2010. *Fossil Behavior Compendium*. 424 pp. CRC Press, London.
- Buikstra, J.E., Cook, D.C., and Bolhofner, K.L. 2017. Introduction: Scientific rigor in paleopathology. *International Journal of Paleopathology* 19: 80–87.
- Checa, A.G., Cartwright, J.H.E., Sánchez-Almazo, I., Andrade, J.P., and Ruiz-Raya, F. 2015. The cuttlefish *Sepia officinalis* Sepiidae, Cephalopoda constructs cuttlebone from a liquid-crystal precursor. *Scientific Reports* 5: 11513.
- Clarke, M.R. 1996. Cephalopods as prey III, Cetaceans. *Philosophical Transactions of the Royal Society of London, Series B* 351: 1053–1065.
- Cremonte, F. and Ituarte, C. 2003. Pathologies elicited by the gymnohalid metacercariae of *Bartolius pierrei* in the clam *Darina solenoides*. *Journal of the Marine Biological Association of the United Kingdom* 83: 311–318.
- Daqué, E. 1921. *Vergleichende biologische Formenkunde der fossilen niederen Tiere*. 777 pp. Borntraeger, Berlin.
- Davis, R.A., Klofak, S.M., and Landman, N.H. 1999. Epizoa on externally shelled cephalopods. In: A.Y. Rozanov and A.A. Shevryev (eds.), *Fossil Cephalopods Recent Advances in Their Study*, 32–52. Russian Academy of Sciences Paleontological Institute, Moscow.
- De Baets, K., Keupp, H., and Klug, C. 2015. Parasites in Ammonoids. In: C. Klug, D. Korn, K. De Baets, I. Kruta, and R.H. Mapes (eds.), *Ammonoid Paleobiology from Anatomy to Ecology. Topics in Geobiology* 43: 837–875.
- De Baets, K., Klug, C., and Korn, D. 2011. Devonian pearls and ammonoid-endoparasite coevolution. *Acta Palaeontologica Polonica* 56: 159–180.
- Dietrich, B., Girod, P., and Schneider, C. 2013. Belemniten. In: C. Schneider (ed.), *Fossilien aus dem Campan von Hannover. Arbeitskreis Paläontologie Hannover Sonderheft*: 143–151.
- d'Orbigny, A. 1842–1851. *Paléontologie française. Description zoologique et géologique de tous les animaux mollusques et rayonnés fossiles de France, comprenant leur application à la reconnaissance des couches. Terrains oolithiques ou jurassiques. Vol. 1. Céphalopodes*. 1–80 (1842), 81–192 (1843), 193–312 (1844), 313–368 (1845), 369–432 (1846), 433–464 (1847), 465–504 (1848), 505–520 (1849), 521–632 (1850), 633–642 (1851). Masson, Paris.
- Doyle, P. 1990. The British Toarcian Lower Jurassic belemnites. *Mono-graph of the Palaeontological Society London* 144: 1–49.
- Duval-Jouve, J. 1841. *Bélemnites des Terrains Crétacés Inférieurs des Environs de Castellane Basses-Alpes considérées Géologiquement et Zoologiquement avec la description de ces Terrains*. 80 pp. Fortin, Masson et cie éditeurs, Paris.
- Engel, T. 1894. Ueber kranke Ammonitenformen im schwäbischen Jura. *Nova Acta Kaiserlich Leopoldinisch-Carolinische Deutsche Akademie der Naturforscher* 61: 326–384.
- Finzel, E. 1963. Der Zweispitz-Belemnit von Misburg – ein Unikum. *Der Aufschluss* 14: 47.
- Fraas, E. 1859. Ueber das Verwachsen von Belemniten. *Jahreshefte des Vereins für vaterländische Naturkunde in Württemberg* 15: 127–128.
- Frerichs, U. 2015. Dokumentation über Belemniten mit Missbildungen aus dem Campan von Höver und Misburg. *Arbeitskreis Paläontologie Hannover* 43: 99–134.
- Fuchs, D. 2012. The “rostrum”—problem in coleoid terminology—an attempt to clarify inconsistencies. *Geobios* 45: 29–39.
- Gestal, C., Pascual, S., Guerra, A., Fiorito, G., and Vieites, J.M. (eds.) 2019. *Handbook of Pathogens and Diseases in Cephalopods*. 230 pp. Springer Open, Heidelberg.
- Götting, K.J. 1979. Durch Parasiten induzierte Perlbildung bei *Mytilus edulis* L. (Bivalvia). *Malacologia* 18: 563–567.
- Hengsbach, R. 1996. Ammonoid pathology. In: N.H. Landman, K. Tanabe, and R.A. Davies (eds.), *Ammonoid Paleobiology. Topics in Geobiology* 13: 581–605.
- Hochberg, F.G. 1990. Diseases in Mollusca Cephalopoda. In: O. Kinne (ed.), *Diseases of Marine Animals, Vol. 3. Cephalopoda to Urochordata*, 21–227. Biologische Anstalt Helgoland, Hamburg.
- Hölder, H. 1956. Über Anomalien an jurassischen Ammoniten. *Paläontologische Zeitschrift* 34: 61–68.
- Hoffmann, R. and Keupp, H. 2015. Ammonoid paleopathology. In: C. Klug, D. Korn, K. De Baets, I. Kruta, and R.H. Mapes (eds.), *Ammonoid aleobiology from Anatomy to Ecology. Topics in Geobiology* 43: 877–926.
- Hoffmann, R. and Stevens, K. 2020. The palaeobiology of belemnites—foundation for the interpretation of rostrum geochemistry. *Biological Reviews* 95: 94–123.
- Hoffmann, R. and Weissmüller, M. 2018. Ein Belemnitenrostrum mit zwei Spitzen aus dem Toarcium Unterjura von Dörlbach bei Altdorf. *Der Steinkern* 34: 38–43.

- Hoffmann, R., Ansoerge, J., Wesendonk, H., and Stevens, K. 2018. A Late Cretaceous pathological belemnite rostrum with evidence of infection by an endoparasite. *Neues Jahrbuch für Geologie und Paläontologie Abhandlungen* 287: 335–349.
- Hoffmann, R., Richter, D.K., Neuser, R.D., Jöns, N., Linzmeier, B.J., Lemanis, R.E., Fousseis, F., Xiao, X., and Immenhauser, A. 2016. Evidence for a composite organic-inorganic fabric of belemnite rostra Implications for palaeoceanography and palaeoecology. *Sedimentary Geology* 341: 203–215.
- Hoffmann, R., Schultz, J.A., Schellhorn, R., Rybacki, E., Keupp, H., Gerden, S.R., Lemanis, R., and Zachow, S. 2014. Non-invasive imaging methods applied to neo- and paleo-ontological cephalopod research. *Biogeosciences* 11: 2721–2739.
- Hüne, L. and Hüne P. 2008. Des phénomènes paléopathologiques chez une faune de Bélemnites du Callovien supérieur de Bénerville-sur-Mer Calvados, France, Calvados, France. *L'Echo des Falaises* 12: 67–70.
- Huntley, J.W. and De Baets, K. 2015. Trace fossil evidence of trematode-bivalve parasite-host interactions in deep time. *Advances in Parasitology* 90: 201–231.
- Ituarte, C.F., Cremonte, F., and Deferrari, G. 2001. Mantle-shell complex reactions elicited by digenean metacercariae in *Gaimardia trapesina* Bivalvia Gaimardiidae from the southwestern Atlantic Ocean and Magellan Strait. *Diseases of Aquatic Organisms* 48: 47–56.
- Jenny, D., Fuchs, D., Arkhipkin, A.I., Hauff, R.B., Fritsch, B., and Klug, C. 2019. Predatory behavior and taphonomy of a Jurassic belemnoid coleoid (Diplobelida, Cephalopoda). *Scientific Reports* 9: 7944.
- Kabanov, G.K. 1967. Skeleton of belemnites. Morphology and biological analysis [in Russian]. *Trudy Paleontologičeskogo Instituta, Akademii Nauk SSSR* 114: 1–117.
- Kauffman, E.G. and Kesling, R.V. 1960. An Upper Cretaceous ammonite bitten by a mosasaur. *Contributions from the Museum of Paleontology, The University of Michigan* 15: 193–148.
- Keupp, H. 2000. *Ammoniten – Paläobiologische Erfolgsspiralen*. 165 pp. Thorbecke, Stuttgart.
- Keupp, H. 2002. Pathologische Belemniten Schein und Wirklichkeit. *Fossilien* 2002 (2): 85–92.
- Keupp, H. 2012. Atlas zur Paläopathologie der Cephalopoden. *Berliner paläobiologische Abhandlungen* 12: 1–390.
- Kinne, O. 1983. Diseases of Mollusca. Introduction to Volume II. In: O. Kinne (ed.), *Diseases of Marine Animals, Vol. 2*, 467–1038. Biologische Anstalt Helgoland, Hamburg.
- Klähn, H. 1925. Die Spaltung des Rostrums von *Belemnitella mucronata* Schl. *Zeitschrift der Deutschen Geologischen Gesellschaft* 77: 93–102.
- Klug, C. 2007. Sublethal injuries in Early Devonian cephalopod shells from Morocco. *Acta Palaeontologica Polonica* 52: 749–759.
- Kraus, W. 2000. Morphologieänderungen von Belemnitenrostrum Phänomene, Ursachen und Bewertung. *Mitteilungen zur Ingenieurgeologie und Hydrogeologie* 76: 119–126.
- Kröger, B. 2000. Schalenverletzungen an jurassischen Ammoniten – ihre paläobiologische und palökologische Aussagefähigkeit. *Berliner Geowissenschaftliche Abhandlungen* 33: 1–97.
- Kröger, B. and Keupp, H. 2004. A paradox survival—report of a repaired syn vivo perforation in a nautiloid phragmocone. *Lethaia* 37: 439–444.
- Landman, N.H. and Waage, K.M. 1986. Shell abnormalities in scaphitid ammonites. *Lethaia* 19: 211–224.
- Lauckner, G. 1983. Diseases of Mollusca Bivalvia. In: O. Kinne (ed.), *Diseases of Marine Animals, Introduction, Bivalvia to Scaphopoda. Vol. 2*, 477–961. Biologische Anstalt Helgoland, Hamburg.
- Lemanis, R., Korn, D., Zachow, S., Rybacki, E. and Hoffmann, R. 2016a. The evolution and development of cephalopod chambers and their shape. *PLoS One* 11: 1–21.
- Lemanis, R., Zachow, S., and Hoffmann, R. 2016b. Comparative cephalopod shell strength and the role of septum morphology on stress distribution. *PeerJ* 4: e2434.
- Lemanis, R., Zachow, S., Fousseis, F., and Hoffmann, R. 2015. A new approach using high-resolution computed tomography to test the buoyant properties of chambered cephalopod shells. *Paleobiology* 41: 313–329.
- Leung, T.L.F. 2017. Fossils of parasites what can the fossil record tell us about the evolution of parasitism? *Biological Reviews* 92: 410–430.
- Littlewood, D.T.J. and Donovan, S.K. 2003. Fossil parasites a case of identity. *Geology Today* 19: 136–142.
- López-González, P., Bresciani, J., Huys, R., González, A., Guerra, A., and Pascual, S. 2000. Description of *Genesi vulcanocopusi* gen. et sp. nov. Copepoda Tibsidiae parasitic on a hydrothermal vent octopod and a reinterpretation of the life cycle of chlidynid harpacticoids. *Cahiers de Biologie Marine* 41: 241–253.
- Meischner, D. 1968. Perniciöse Epökie von *Placunopsis* auf *Ceratites. Lethaia* 1: 156–174.
- Miertzsch, E. 1964. Ein Belemnit mit fünf Spitzen. *Der Aufschluss* 15: 74.
- Mietchen, D., Keupp, H., Manz, B., and Volke, F. 2005. Non-invasive diagnostics in fossils—Magnetic Resonance Imaging of pathological belemnites. *Biogeosciences* 2: 133–140.
- Moosleitner, G. 2006. Meeresleben in der Unteren Kreide. Die Valanginiummergel im Raum Salérans Col d'Araud. *Fossilien* 2006 (2): 79–86.
- Moosleitner, G. 2012. Fossilien sammeln in der Provence Die Unterkreide des Plan du Peyron. *Fossilien* 2012 (3): 176–184.
- Monks, N., Hardwick, J.D., and Gale, A.S. 1996. The function of the belemnite guard. *Paläontologische Zeitschrift* 70: 425–431.
- Ozanne, C.R. and Harries, P.J. 2002. Role of predation and parasitism in the extinction of the inoceramid bivalves an evaluation. *Lethaia* 35: 1–19.
- Pascual, S., Gestal, C., Estévez, J.M., Rodríguez, H., Soto, M., Abollo, E., and Arias, C. 1996. Parasites in commercially-exploited cephalopods Mollusca, Cephalopoda in Spain an updated perspective. *Aquaculture* 142: 1–10.
- Pascual, S., González, A., and Guerra, A. 2007. Parasites and cephalopod fisheries uncertainty towards a waterfall understanding. *Revue of Fish Biology and Fisheries* 17: 139–144.
- Poulin, R. 2011. The many roads to parasitism a tale of convergence. *Advances in Parasitology* 74: 1–40.
- Quenstedt, F.A. 1846–1849. *Petrefaktenkunde Deutschlands. Erste Abtheilung, Band 1, Die Cephalopoden*. 581 pp. Friedrich Ludwig Fues, Tübingen.
- Quenstedt, F.A. 1858. *Der Jura*. 407 pp. Schweizerbart, Tübingen.
- Radwańska, U. and Radwański, A. 2004. Disease and trauma in Jurassic invertebrate animals of Poland—an updated review. *Volumina Jurassica* 2: 99–111.
- Raspail, F.V. 1829. Histoire naturelle des Bélemnites, accompagnée de la description et de la classification des espèces que M. Éméric, de Castellane, a recueillies dans les Basses Alpes de provence. Première Partie. *Annales Des Sciences D'Observation* 1: 271–331.
- Richter, A.E. 1993. Die Belemniten – eine “langweilige Gesellschaft”. *Fossilien* 1993 (4): 227–236.
- Richter, A.E. 2009. Ammoniten-Gehäuse mit Bisspuren. *Berliner Paläobiologische Abhandlungen* 10: 297–305.
- Richter, D.K., Neuser, R.D., Schreuer, J., Gies, H., and Immenhauser, A. 2011. Radial-fibrous calcites A new look at an old problem. *Sedimentary Geology* 239: 23–36.
- Rita, P., De Baets, K., and Schlott, M. 2018. Rostrum size differences between Toarcian belemnite battlefields. *Fossil Record* 21: 171–182.
- Ruiz, G.M. and Lindberg, D.R. 1989. A fossil record for trematodes extent and potential uses. *Lethaia* 22: 431–438.
- Schindewolf, O.H. 1934. Über Epöken auf Cephalopoden-Gehäusen. *Paläontologische Zeitschrift* 16: 15–31.
- Schlüter, C.A. 1876. Cephalopoden der oberen deutschen Kreide-Teil 3. *Palaeontographica* 24: 123–204, 207–263.
- Schmid, F. 1963. Ein Nachtrag zum “Zweispitz-Belemnit” aus dem Unter-campan von Misburg bei Hannover, pathologische Ausbildung an *Gontoteuthis quadrata* Blainville. *Der Aufschluss* 14: 294–296.
- Schröter, J.S. 1774. Abhandlung von den Ammoniten der Weimarischen Gegend. *Der Naturforscher* 2. Stück, 177 pp.
- Schwegler, E. 1939. Eine merkwürdige Krankheitserscheinung bei einem Belemniten aus dem Braunen Jura zeta Schwabens und ihre Deutung.

- Zentralblatt für Mineralogie, Geologie und Paläontologie Abteilung B* 1939: 74–80.
- Seilacher, A. 1968. Swimming habits of belemnites—recorded by boring barnacles. *Palaeogeography, Palaeoclimatology, Palaeoecology* 4: 279–285.
- Seilacher, A. and Gishlick, A.D. 2015. *Morphodynamics*. 531 pp. CRC Press, Boca Raton.
- Shufeldt, R.W. 1892. Notes on palaeopathology. *Popular Science Monthly* 1892: 679–684.
- Stevens, K., Griesshaber, E., Schmahl, W., Casella, L.A., Iba, Y., and Mutterlose, J. 2017. Belemnite biomineralization, development, and geochemistry. The complex rostrum of *Neohibolites minimus*. *Palaeogeography, Palaeoclimatology, Palaeoecology* 468: 388–402.
- Tasnadi-Kubacska, A. 1962. *Paläopathologie – Pathologie der vorzeitlichen Tiere*. 269 pp. VEB Gustav Fischer Verlag, Jena.
- Thomel-Picollier, M.-C. 2018. *Etude d'une population de Bélemnites du genre Pseudobelus du Crétacé inférieur dans le Sud-Est de la France*. 49 pp. Published online by the author at <http://www.cephalopodes-cretaces.com/pages/belemnite/le-genre-pseudobelus/>
- Tsujino, Y. and Shigeta, Y. 2012. Biological response to experimental damage of the phragmocone and siphuncle in *Nautilus pompilius* Linnaeus. *Lethaia* 45: 339–449.
- Vallon, L.H., Rindsberg, A.K., and Martin, A.J. 2015. The use of the terms trace, mark and structure. *Annales Societatis Geologorum Poloniae* 85: 527–528.
- Weissmüller, M. 2017. *Eine Reise in den unteren Jura der Region Altdorf*. 200 pp. Published by the author, Berg.
- Wisshak, M., Titschack, J., Kahl, W.-A., and Girod, P. 2017. Classical and new bioerosion trace fossils in Cretaceous belemnite guards characterised via micro-CT. *Fossil Record* 70: 173–199.
- Wundt, G. 1883. Ueber die Vertretung der Zone des *Ammonites transversarius* im schwäbischen weissen Jura. *Jahreshefte des Vereins für vaterländische Naturkunde in Württemberg* 39: 148–165.
- Ziegler, A., Bock, C., Ketten, D.R., Mair, R.W., Mueller, S., Nagelmann, N., Pracht, E.D., and Schröder, L. 2018. Digital three-dimensional imaging techniques provide new analytical pathways for malacological research. *American Malacological Bulletin* 36: 248–273.